Developmental Biology **232,** 372–387 (2001)
doi:10.1006/dbio.2001.0200, available online at http://www.idealibrary.com on IDEAL®

A Novel Chordin-like Protein Inhibitor for Bone Morphogenetic Proteins Expressed Preferentially in Mesenchymal Cell Lineages

Naoki Nakayama,*[,1] Chun-ya E. Han,* Sheila Scully,† Ryuichi Nishinakamura,‡ Ching He,* Lisa Zeni,§ Harvey Yamane,§ David Chang,* Dongyin Yu,* Takashi Yokota,‡ and Duanzhi Wen*

**Department of Cell Biology, †Department of Pathology, and §Department of Protein Chemistry, Amgen Incorporated, One Amgen Center Drive, Thousand Oaks, California 91320; and ‡Department of Stem Cell Regulation, Institute of Medical Science, The University of Tokyo, 4-6-1 Shirokanedai, Minato-ku, Tokyo 108, Japan*

Chordin is a bone morphogenetic protein (BMP) inhibitor that has been identified as a factor dorsalizing the *Xenopus* embryo. A novel secreted protein, CHL (for chordin-like), with significant homology to chordin, was isolated from mouse bone marrow stromal cells. Injection of CHL RNA into *Xenopus* embryos induced a secondary axis. Recombinant CHL protein inhibited the BMP4-dependent differentiation of embryonic stem cells *in vitro* and interacted directly with BMPs, similar to chordin. However, CHL also weakly bound to TGFβs. *In situ* hybridization revealed that the mouse CHL gene, located on the X chromosome, was expressed predominantly in mesenchyme-derived cell types: (1) the dermatome and limb bud mesenchyme and, later, the subdermal mesenchyme and the chondrocytes of the developing skeleton during embryogenesis and (2) a layer of fibroblasts/connective tissue cells in the gastrointestinal tract, the thick straight segments of kidney tubules, and the marrow stromal cells in adults. An exception was expression in the neural cells of the olfactory bulb and cerebellum. Interestingly, the spatiotemporal expression patterns of CHL were distinct from those of chordin in many areas examined. Thus, CHL may serve as an important BMP regulator for differentiating mesenchymal cells, especially during skeletogenesis, and for developing specific neurons.

Key Words: **secreted protein; chordin; BMP inhibitor; embryogenesis; embryonic stem cell; dorsalizing factor; skeletogenesis; mesenchymal cell; chondrocyte; organogenesis.**

INTRODUCTION

Bone morphogenetic proteins (BMPs) belong to the transforming growth factor (TGF)β superfamily and were originally identified as factors promoting the ectopic formation of cartilage and bone (reviewed in Wang, 1993). BMPs are also known to play an essential role during the early embryogenesis of *Drosophila*, *Xenopus*, zebrafish, and mammals (reviewed in Harland and Gerhart, 1997). Moreover, BMPs are involved in cell-type specification during the organogenesis phase of embryogenesis (reviewed in Hogan, 1996). In any case, BMPs are pleiotropic factors, and the precise concentration of active BMP seems to be important for rendering a particular biological effect. In fact, an activity gradient of BMP is formed during embryogenesis in *Drosophila* as well as in *Xenopus*, which leads to the generation of different cell types, depending on the location (i.e., the local BMP concentration) (reviewed in Dale and Wardle, 1999; Podos and Ferguson, 1999).

The active BMP concentration is controlled in part through the influence of BMP inhibitors. Several BMP binding proteins have been described: short gastrulation/chordin (Francois *et al.*, 1994; Pappano *et al.*, 1998; Sasai *et al.*, 1994; Schulte-Merker *et al.*, 1997), noggin (Smith and Harland, 1992; Zimmerman *et al.*, 1996), and cerberus (Belo *et al.*, 1997; Biben *et al.*, 1998; Bouwmeester *et al.*, 1996). Among them, chordin and noggin are known to inhibit the

[1] To whom correspondence and reprint requests should be addressed at Department of Cell Biology, Inflammation Research, Amgen Inc., MS: 14-1-D, One Amgen Center Drive, Thousand Oaks, CA 91320. Fax: 1-805-447-1982. E-mail: naoki.nakayama@amgen.com.

0012-1606/01 $35.00

activity of bound BMP by preventing it from binding to its receptor (Piccolo *et al.,* 1996; Zimmerman *et al.,* 1996). Chordin is a secreted protein produced from the Spemann's organizer of the *Xenopus* embryo and functions as a dorsalization factor by antagonizing the ventralizing factor, BMP4. The binding affinity of chordin to BMP4 is specific and tight (Piccolo *et al.,* 1996), and proteolysis seems to be required to effectuate the release of bound BMP4. The chordin polypeptide contains four cysteine-rich units designated procollagen repeats (CRs), which are also found in a variety of extracellular matrix proteins, such as collagen and thrombospondin. The first and third CRs (CR1 and CR3) of chordin are responsible for BMP binding (Larrain *et al.,* 2000). Proteolytic degradation of chordin is accomplished by a metalloprotease, Tolloid or BMP1, that liberates both CR1 and CR4 (Piccolo *et al.,* 1997; Scott *et al.,* 1999).

It is conceivable that, if expressed at the same time and location, any of the BMP binding inhibitors would functionally compensate for each other. This is the case for chordin and noggin in the mouse (Bachiller *et al.,* 2000; Brunet *et al.,* 1998; McMahon *et al.,* 1998). Mouse chordin mRNA is first detected in the anterior primitive streak and then in the node and axial mesoderm. At the midgastrula stage, chordin expression overlaps with that of noggin. Mutational analyses have shown that the early embryonic functions of chordin and noggin are individually dispensable for embryonic development. However, chordin is essential for inner and outer ear development as well as for pharyngeal and cardiovascular organization (Bachiller *et al.,* 2000). Similarly, noggin null-mutant mice display multiple developmental defects occurring at late stages of embryogenesis, including limb and digit defects caused by chondrocyte hyperplasia (Brunet *et al.,* 1998; McMahon *et al.,* 1998). In contrast, double mutants show early embryonic phenotypes (Bachiller *et al.,* 2000). Thus, these BMP inhibitors seem to share biological roles during early embryogenesis, whereas the roles of the individual inhibitors become specialized in later stages of development, so that some functions of chordin are no longer compensated by noggin or other BMP inhibitors.

Functional redundancy often occurs in members of the same gene family. Cerberus is known to form a large gene family: cerberus/Cer1 (Biben *et al.,* 1998; Bouwmeester *et al.,* 1996; Shawlot *et al.,* 1998), DAN (Ozaki *et al.,* 1996; Stanley *et al.,* 1998), Gremlin/Drm (Hsu *et al.,* 1998; Topol *et al.,* 1997), and Dte (Pearce *et al.,* 1999). It has recently been shown that noggin also forms a family in zebrafish (Fuerthauer *et al.,* 1999). However, thus far, no functional redundancy has been demonstrated within these families. On the contrary, differences in the spatial as well as temporal order of expression during embryogenesis have been demonstrated, suggesting a different biological role for each member of the family. In the case of zebrafish noggin, noggin1 is expressed earliest and is active in dorsalizing the embryo, while noggin3 is the latest expressing member and probably functions during organogenesis. Recently, a large secreted *Xenopus* protein containing 27 CRs, which shows chordin-like dorsalizing activity in *Xenopus* embryos, was identified (Matsui *et al.,* 2000). Here, we provide evidence that a novel chordin family member, CHL (for chordin-like), is a BMP inhibitor, and the gene is localized on the X chromosome and is expressed preferentially in mesenchymal cell lineages with spatial and temporal patterns distinct from those of chordin. Potential roles of CHL during several organogenic processes are also discussed.

MATERIALS AND METHODS

Cells and reagents. Polymerase chain reaction (PCR) and cDNA synthesis were performed with Advantage Taq (Clontech, Palo Alto, CA) and the Superscript cDNA library kit (Gibco/BRL, Gaithersburg, MD), respectively, according to the manufacturer's recommendations. Other enzymes were purchased from New England BioLabs (Beverly, MA) or Boehringer Mannheim (Indianapolis, IN). The human erythropoietin (EPO) cDNA was kindly provided by S. Wooden (Amgen).

The E14 ES cells and the OP9 stromal cell line were obtained and cultured as described (Nakayama *et al.,* 1998, 2000). The human kidney epithelial cell lines, 293 and 293T, were maintained in Dulbecco's modified essential medium (DMEM, Gibco/BRL) supplemented with 10% fetal calf serum (FCS, Hyclone, Logan, UT) at 37°C under 5% CO_2. All tissue culture flasks and plates were from Falcon (Franklin Lakes, NJ).

Recombinant human BMP4, BMP5, BMP6, activin A, TGFβ2, and BMPR1BFc were purchased from R&D Systems (Minneapolis, MN). The corresponding antibodies used for Western blot detection were the anti-human BMP4 mouse monoclonal antibody from Chemicon (Temecula, CA), the anti-human BMP5 goat polyclonal antibody from R&D, the anti-human BMP6 mouse monoclonal antibody from Chemicon, the anti-human activin A goat polyclonal antibody from R&D, and the anti-human TGFβ2 goat polyclonal antibody from R&D. A human IgG Fc control was obtained from Zymed (South San Francisco, CA). The monoclonal antibody for mouse CD34 (clone RAM34) conjugated with fluorescein isothiocyanate (FITC) was purchased from Pharmingen (San Diego, CA). Phycoerythrin (PE)-conjugated monoclonal antibodies for mouse CD31 (clone MEC13.3) and CD45 (clone 30F11) were also purchased from Pharmingen.

Isolation of mouse CHL cDNAs. Normalized cDNAs were prepared with poly(A)$^+$ RNA isolated from OP9 cells according to the PCR-based normalization procedure (Takahashi and Ko, 1994). Small fragments (500–1000 bp) were used to construct a library for yeast-based signal sequence trap screening (Jacobs *et al.,* 1997; Klein *et al.,* 1996). An unnormalized cDNA library was also constructed in pSPORT1 (Gibco/BRL). From one pool of the normalized OP9 library (3×10^5 independent clones) screened, a cDNA fragment encoding a putative NH_2-terminal amino acid sequence of a protein with significant homology to chicken chordin, which was designated CHL, was identified by a Blast search (Genomics Computer Group, Madison, WI). Using this partial cDNA as a probe, the corresponding full-length cDNA clone, mCHL(s2), was isolated from the unnormalized cDNA library (pSPORTmCHL(s2)). Furthermore, another cDNA clone designated mCHL(l3) that potentially encoded a different form of CHL was isolated from the mouse E15.5 embryo library (GIBCO/BRL). For stable expression, the full-length mCHL(s2) cDNA was

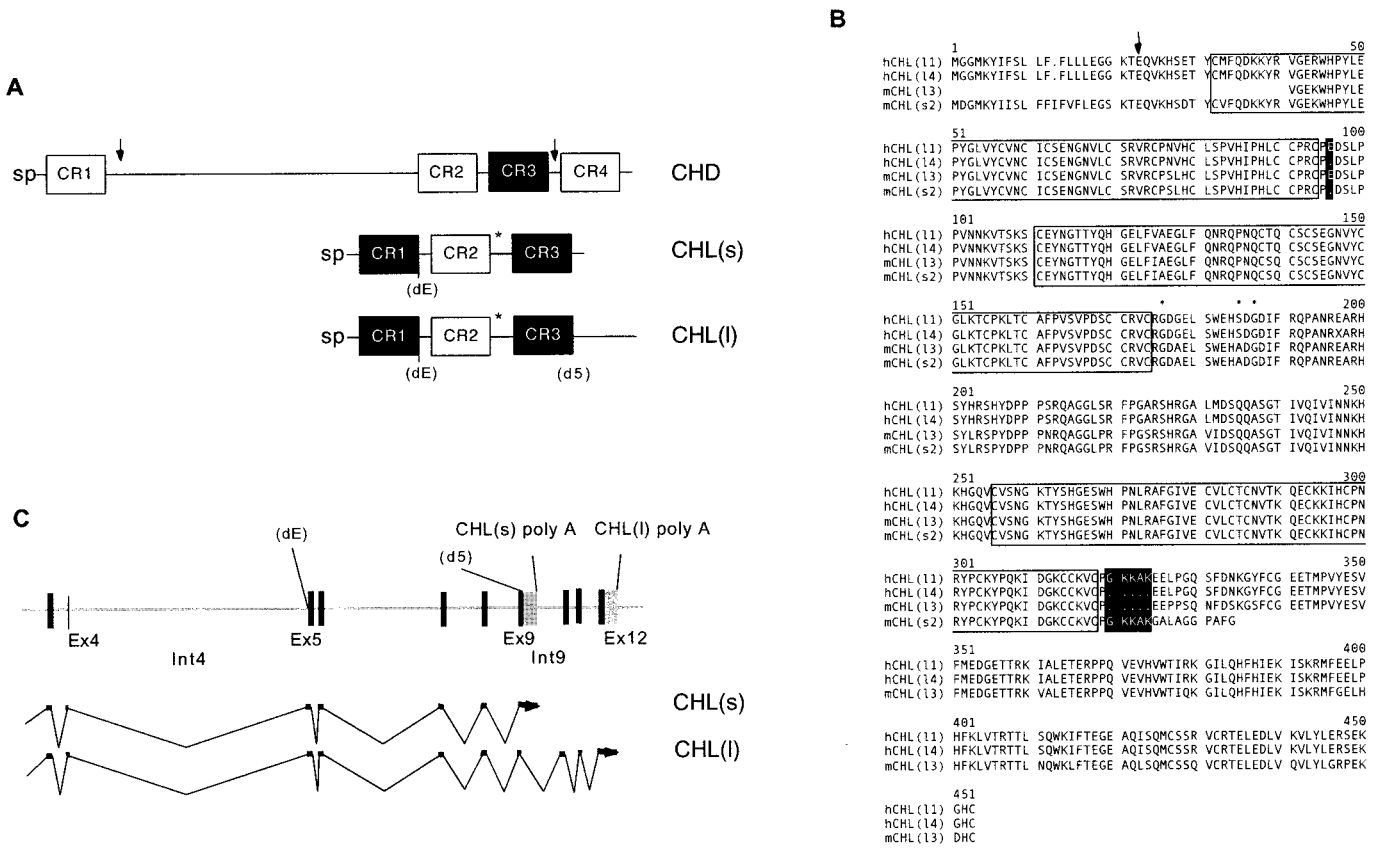

FIG. 1. Schematic representation of CHL and chordin gene products. (A) Schematic representation of mouse CHL (CHL(s) and CHL(l)) and chordin (CHD) gene products. CR and SP stand for the procollagen repeat and the signal peptide, respectively. The cluster of putative BMP1/Tolloid cleavage sites is indicated with an asterisk. The CR1 and CR3 in mouse CHL are homologous with CR3 of mouse chordin, indicated with black boxes. The two sites, at which amino acid sequence variations were found in the CHL ORF, are shown by dE and d5 in parentheses. The dE indicates $E^{95/96}$ missing in the l2, l4, and s2 forms of CHL, and d5 indicates the GKKAK sequence deleted in the l3 and l4 forms. (B) Amino acid sequences of the human CHL(l1) and CHL(l4) and mouse CHL(l3) and CHL(s2) protein precursors. The three CRs are indicated as boxes. The E^{23} indicated by the vertical arrow was determined as the NH_2-terminal amino acid of the mature mCHL(s2)-FLAG protein. The amino acid with an asterisk corresponds to the potential BMP1/Tolloid cleavage site. The $E^{95/96}$ missing in hCHL(l4) as well as in mCHL(s2) and the GKKAK stretch deleted in hCHL(l4) are indicated with black backgrounds. (C) Schematic representation of the partial intron–exon structure of the hCHL gene and transcripts. The top is the partial genomic organization based on AL049176. The vertical bars are exons, which correspond to thick horizontal bars/arrows in the two potential CHL transcripts shown underneath (CHL(s) and CHL(l)). The thin lines of the transcripts indicate splicing. The $E^{95/96}$ deletion mutation, indicated as dE, is created by an alternative splicing acceptor at the junction of intron 4 (Int4) and exon 5 (Ex5). The GKKAK deletion mutation, indicated as d5, is generated at the junction between exon 9 (Ex9) and intron 9 (Int9). The gray vertical bar in intron 9 indicates the region corresponding to the 3′-UTR of the CHL(s) transcript.

cloned into pcDNA3.1 (Invitrogen, Carlsbad, CA) to obtain pcDNAmCHL(s2), and for transient expression, the same cDNA was cloned into an SRα-based expression plasmid (Takebe *et al.*, 1988) to yield pSRαmCHL(s2). As a negative control, pSRαhEPO carrying the human EPO cDNA in place of mCHL(s2) was also constructed.

Isolation of human CHL cDNAs. Total RNA was isolated from rat prostate, poly(A)$^+$ RNA was purified, and normalized cDNA inserts were prepared as described above. A longer range of cDNAs (> 1000 bp) was used to construct a cDNA library for expression sequence tag (EST) analysis (Adams *et al.*, 1991). A sequence containing a partial ORF almost identical to that of the mCHL cDNA was identified and was used as a probe to isolate full-length human CHL cDNAs. Screening of human prostate and fetal brain cDNA libraries (Stratagene, La Jolla, CA) resulted in four different forms of human CHL cDNAs, designated hCHL(l1) to hCHL(l4). All were cloned into pcDNA3.1 to yield pcDNAhCHL(l1), pcDNAhCHL(l2), pcDNAhCHL(l3), and pcDNAhCHL(l4). To construct hCHL(s1) and hCHL(s2), the exon-9–intron 9 boundary region was first amplified by PCR with the sense primer 5′-AGCAAGAGTGTAAGAAAATCCAC-3′ and the antisense primer 5′-AGAATCTCAGTCAACCAAAAGC-3′ using human genomic DNA as the template. The amplified fragment was then cloned into pCR II-TOPO (Invitrogen), excised with *Cla*I and *Not*I, and transferred

to the *Cla*I–*Not*I sites of pcDNAhCHL(l1) and pcDNAhCHL(l2) to obtain pcDNAhCHL(s1) and pcDNAhCHL(s2), respectively.

Construction of the FLAG-tagged mouse CHL(s2) and chordin: mCHL(s2)-FLAG and mCHD-FLAG. The mCHL(s2) ORF was mutated to replace the stop codon with a *Bam*HI site by PCR using the sense primer 5′-GCTAGCGGCCGCGCCACCATGGATGG-CATGAAATACATCATTTC-3′ and the antisense primer 5′-GGTACCGGATCCACCAAAGGCAGGGCCTCCAGC-3′. The amplified DNA fragment was digested with *Not*I and *Bam*HI and was then inserted into the *Not*I–*Bam*HI sites of the pFLAG-CMV-5a expression vector (Sigma) to attach the FLAG sequence in frame with the mCHL(s2) sequence at its COOH-terminus (mCHL(s2)-FLAG). The resultant plasmid was designated pFLAG-mCHL(s2).

Next, mouse chordin cDNA was isolated by reverse transcriptase (RT)–PCR from the mouse E7 embryo cDNAs (Clontech, Palo Alto, CA) using the sense primer 5′-GCTAGCGGCCGCGCC-ACCATGCCGAGCCTCCCGGCCCCG-3′ and the antisense primer 5′-GGATCCGTCGACGGAGTGCTCCGCTTCTTTCTC-CAG-3′. The amplified PCR product was digested with *Not*I and *Sal*I and was then inserted into the *Not*I–*Sal*I sites of pFLAG-CMV-5a, which resulted in a COOH-terminal FLAG fusion protein of the mouse chordin (mCHD-FLAG), to yield pFLAGmCHD.

Production and detection of the recombinant mouse CHL(s2) and chordin proteins. The FLAG-tagged proteins were detected by direct Western blot analysis with 10 μg/ml of the anti-FLAG mouse monoclonal antibody M2 (Sigma), according to the manufacturer's recommendations. Rabbit polyclonal antibodies for mCHL and mouse chordin were raised with synthetic peptides based on the NH_2-terminal amino acid sequences of their presumptive mature proteins: NH_2-SKTEQVKHSDTYC-COOH for mCHL and NH_2-ALPIRSEKEPLPVRGAAGC-COOH for chordin (Harlow and Lane, 1988). The resulting antisera were either used directly or subjected to affinity purification with the corresponding peptides (Harlow and Lane, 1988).

To establish cell lines stably expressing the mCHL(s2)-FLAG or mCHD-FLAG protein, 293 cells were transfected with linearized pFLAGmCHL(s2) or pFLAGmCHD mixed with linearized pKJ1 (Adra *et al.*, 1987), using the calcium phosphate method (Sambrook *et al.*, 1989). Stable transfectants were then selected in 570 μg/ml G418 (Gibco/BRL). The expression levels of the corresponding FLAG-tagged protein, in both the serum-free conditioned media (DMEM, 48 h) and the cell lysates, were compared by Western blot analysis using the M2 antibody or the affinity-purified anti-NH_2-terminal peptide antibody (diluted 1:500 to 1:1000) (Harlow and Lane, 1988). Conditioned media were concentrated 10-fold by Centricon ultrafiltration (Millipore, Bedford, MA) before Western blotting. The proteins were visualized with peroxidase-conjugated anti-mouse or anti-rabbit IgG secondary antibody (Pierce, Rockford, IL) and the chemiluminescent ECL kit (Amersham/Pharmacia, Piscataway, NJ).

Similarly, transient transfection-based expression was carried out with 293T cells using the SuperFect transfection reagent (Qiagen, Valencia, CA) according to the manufacturer's suggested protocol. Twenty-four hours later, the medium was changed to serum-free media, such as 293 SFM II (Gibco/BRL), DMEM, and DMEM with 50 μg/ml iron-saturated human transferrin (Sigma) and 10 μg/ml bovine insulin (Boehringer Mannheim), and the cells were cultured for another 48 h. Tenfold concentrated conditioned media were then analyzed by Western blotting.

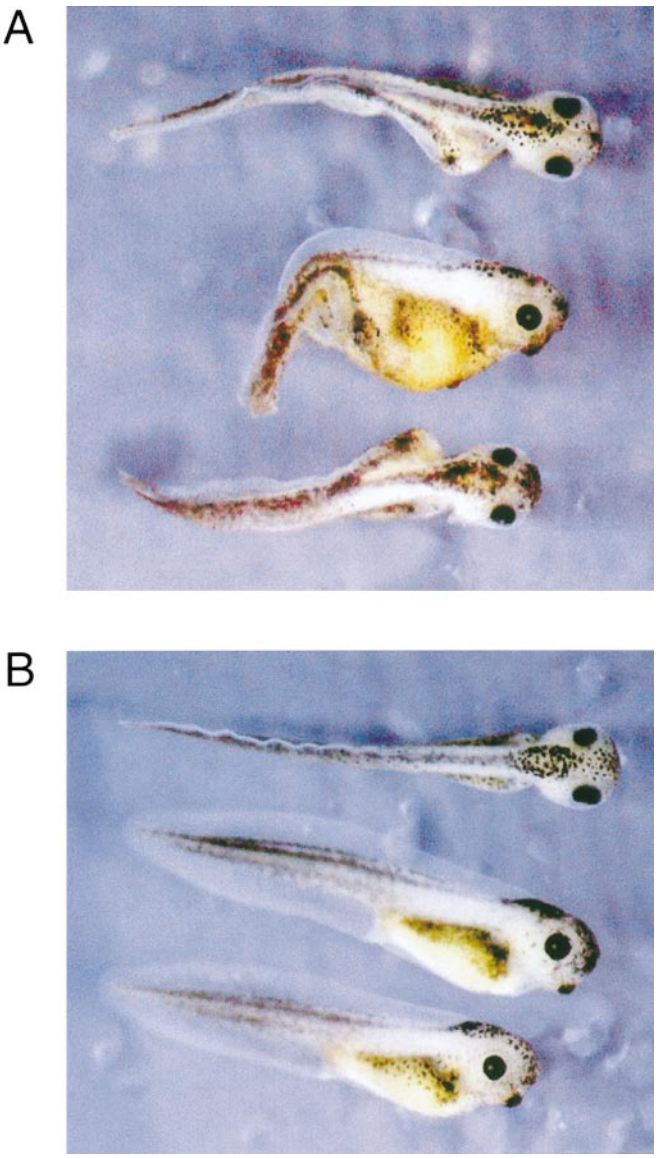

FIG. 2. Secondary axis formation by mCHL(s2). Injection of 30 pg of each RNA made *in vitro* from pcDNAmCHL(s2) into two blastomeres of four-cell stage *Xenopus* embryos resulted in axis duplication in 48 h (A). In contrast, uninjected embryos showed normal development (B).

Partial purification of the FLAG-tagged mouse CHL(s2) and chordin proteins. For midscale preparation, the stable clones were expanded in suspension using 293 SFM II in a 3-liter spinner flask, and 3-day conditioned media for mCHL(s2)-FLAG and 6-day conditioned media for mCHD-FLAG were collected. An expression level of approximately 0.1–0.2 μg/ml was obtained. The FLAG-tagged proteins were partially purified by a single step of affinity chromatography using the anti-FLAG M2 affinity gel (Sigma) according to the manufacturer's recommendations. The protein concentration of each preparation was determined by Western blot

TABLE 1
Secondary Axis Formation by Different Forms of CHL

Type of CHL injected	Embryos with axis duplication/total injected embryos (%)				
	0	10	30	1000	pg RNA/blastomere
Uninjected	0/31 (0)				
EF1				0/23 (0)	
mCHD-FLAG[a]				19/23 (83)	
mCHL(s2)		20/26 (77)	26/30 (87)		
mCHL(s2)-FLAG[b]			15/19 (79)		
hCHL(l1)				19/41 (46)	
hCHL(l2)				13/34 (38)	
hCHL(s1)				15/37 (41)	
hCHL(s2)				33/40 (83)	

[a] pBluescript (SK^+) vector background.
[b] pBluescript RN3 vector background.

analysis with M2 and comparison with the FLAG bacterial alkaline phosphatase standard (Sigma).

Co-immunoprecipitation analysis. Immunoprecipitation was performed as described (Piccolo *et al.*, 1996). Briefly, for the high concentration conditions, 0.4 μg mCHL(s2)-FLAG or 1.2 μg mCHD-FLAG was mixed with 0.2 μg of BMP, activin A, or TGFβ2 in 1 ml of binding buffer, and the solution was incubated for 1 h at 4°C. Then, either 1.5–4 μg of affinity-purified anti-peptide antibody or 40 μl of crude antisera was added, and the solution was incubated for another 1 h. Next, 20 μl protein A or 30 μl of protein A/G plus agarose beads (Santa Cruz) was added, and the mixture was incubated for another 3 h to overnight. For the low concentration conditions, 0.1 μg of mCHL(s2)-FLAG or 0.3 μg of mCHD-FLAG was mixed with 90–100 ng of BMP or activin A, and the reaction was processed in the same way. To demonstrate the role of CHL in BMP4 binding to the BMP receptor (BMPR), 100 ng of BMP4 and various amounts of mCHL(s2)-FLAG were mixed in 1 ml of binding buffer, and then 1 μg of BMPR1BFc or IgG Fc was added. The resulting BMPR complex was precipitated directly with 20 μl of protein A beads. The isolated immunocomplexes were electrophoresed through SDS–polyacrylamide gels under reducing conditions and then were blotted onto nitrocellulose membranes. The filter was treated with 0.4 μg/ml anti-BMP4, 0.1 μg/ml anti-BMP5, 0.1 μg/ml anti-BMP6, 0.4 μg/ml anti-activin A, or 1 μg/ml anti-TGFβ2 antibody for 2 h at room temperature, and the bound antibodies were visualized as described.

Ectopic axis formation in Xenopus embryo. To examine the mouse and human CHL protein activities, pcDNAmCHL(s2), pcDNAhCHL(l1), pcDNAhCHL(l2), pcDNAhCHL(s2), and pcDNAhCHL(s2) were linearized with *Not*I, and capped mRNAs were synthesized with T7 RNA polymerase using the mMESSAGE mMACHINE kit (Ambion, Austin TX) and were quantified as described (Nishinakamura *et al.*, 1999). For mCHL(s2)-FLAG, the *Eco*RI–*Sca*I fragment of pFLAGmCHL(s2) was cloned into the *Eco*RI–*Not*I sites of pBluescript RN3 (Lemaire *et al.*, 1995), linearized with *Sfi*I, and transcribed with T3 RNA polymerase using the mMESSAGE mMACHINE kit. For mCHD-FLAG, the *Not*I–*Sca*I fragment of pFLAGmCHD was introduced into the *Not*I–*Sma*I sites of the pBluescript (SK^+) vector (Stratagene), which was then linearized with *Cla*I and transcribed in the same way. As a negative control, elongation factor 1 (EF1) RNA was synthesized using the template included in the kits. *Xenopus* embryos were also prepared for injection as described (Nishinakamura *et al.*, 1999). Five nanoliters of each RNA was injected into two ventral blastomeres of a four-cell stage embryo. After the injection, the embryos were cultured in 10% Steinberg's solution for 48 h and were then scored for the ectopic axis.

In vitro differentiation of embryonic stem cells under serum-free conditions. Briefly, E14 embryonic stem (ES) cells were transferred to a gelatin-coated plate, adjusted for 2 days in serum-free medium, and then subjected to differentiation in serum-free methylcellulose medium in the presence of 0.6 ng/ml BMP4 as described (Nakayama *et al.*, 2000). Embryoid bodies were collected on day 7 and were dissociated with collagenase. The cells were stained with monoclonal antibodies for hematopoietic progenitor cell markers, such as CD31, CD34, and CD45, as described (Nakayama *et al.*, 2000). The stained samples were analyzed on a FACScan (Becton–Dickinson, San Jose, CA).

In situ hybridization and Northern blot analyses. Northern blotting was performed (Sambrook *et al.*, 1989) with multiple mouse tissue Northern blots purchased from Clontech, using the ^{32}P-labeled *Not*I–*Bam*HI fragment from pFLAGmCHL(s2) that contained the entire ORF of mCHL(s2) as a probe. The chordin transcript was detected on the same blots with the ^{32}P-labeled *Not*I–*Sal*I fragment from pFLAGmCHD containing the intact ORF of mouse chordin. For detecting the mCHL(s)-specific transcripts, a probe (designated the intron 9 probe) was made by PCR with the primers 5′-CCTGCCTTTGGTTGAATGAG-3′ and 5′-GGAGATAGAGGTTAGATAGTAG-3′, which were derived from the nucleotide sequence of the 3′-untranslated region (UTR) of the mCHL(s2) cDNA.

In situ hybridization to embryonic and adult mouse tissue sections was carried out according to Wilcox (1993). For the CHL probe, the *Cla*I–*Not*I region of pSPORTmCHL(s2) was removed to obtain pSPmCHL5′, which was then linearized with *Eco*RI. The antisense RNA was synthesized with SP6 RNA polymerase. For chordin, the 1.4-kb *Bam*HI–*Bgl*II fragment of pFLAGmCHD was transferred into the *Bam*HI site of the pBluescript (SK^-) vector (Stratagene), which was linearized with *Eco*RI. The antisense RNA was synthesized with T3 RNA polymerase.

Cloning of the mouse CHL gene and the chromosomal localization. The chromosomal location of the mouse CHL gene was determined by Genome Systems, Inc. (St. Louis, MO), using the fluorescence *in situ* hybridization (FISH) technique of Shi *et al.* (1997). The probe was a BAC clone, F1038, isolated from the mouse ES-129/SvJ II BAC chromosome DNA library (Genome Systems) by PCR using the sense primer 5′-TTACCACCAGTGAAC-AATAAGG -3′ and the antisense primer 5′-CTTGAGACCAC-AGTATACATTCC-3′, which correspond to the second CR domain of mCHL(s2), and with the sense primer 5′-AGTG-CCCAGCTTTAGTCCAC-3′ and the antisense primer 5′-GTT-CTGTTTTGCTTCCTTCTAG-3′, which cover the 5′-UTR and the signal peptide region. To determine the location of the mouse CHL gene on the X chromosome, the X centromere-specific P1 clone (No. 6856) was also used as a cohybridization probe (Shi *et al.*, 1997). A total of 80 metaphase cells were analyzed, and of the 72 that exhibited specific labeling,10 were used for cohybridization experiments.

RESULTS

Cloning of a cDNA Encoding a Novel Chordin-like Gene Product from the Mouse Bone Marrow Stromal Cell Line OP9

The OP9 stromal cell genomics resulted in a cDNA encoding a 333-amino-acid protein precursor consisting of a potential signal peptide followed by three CRs similar to the chordin CRs. The homology with the chordin CRs ranged from 40 to 53% by a Blast search, which was statistically significant compared with the CRs of other proteins, such as thrombospondin and collagen (data not shown). Therefore, the predicted protein was designated CHL for chordin-like (Fig. 1A). During the course of the full-length mouse CHL (mCHL) cDNA cloning, a partial clone encoding a variant of mCHL was identified from an E15.5 mouse embryo cDNA library. This had an insertion of one glutamate residue at position 96 (E^{96}) and carried a longer COOH-terminal sequence (Fig. 1B). Assuming that both forms share the same 5′-end sequence, the predicted full-length ORF would consist of 448 amino acids, which is larger than the first form. Human CHL (hCHL) cDNAs were also isolated, and all of them resembled the longer form of mCHL. A sequence analysis indicated that there were small deletions at two sites within the coding region, which would make four different hCHL products (Fig. 1B). The longest encoded a protein of 452 amino acids and was designated hCHL(l1). The suffix "l" in parentheses stands for the long form, and "1" stands for no deletion. At one site, one amino acid, E^{95}, was missing, which gave rise to a 451-amino-acid protein (hCHL(l2)). At the other site, a 15-bp segment encoding G^{319}-K-K-A-K^{323} was missing, which resulted in a 447-amino-acid protein (hCHL(l3)). A double mutant was also obtained (hCHL(l4)). The suffix "2" means the deletion of E^{95}(E^{96} in mice), "3" stands for the deletion of the GKKAK stretch, and "4" corresponds to mutations at both sites. Therefore, the original mouse clone was renamed mCHL(s2), in which the suffix "s" in parentheses stands for the short form, and the second mouse clone was designated mCHL(l3). CHL(l) and CHL(s) represent the long forms and the short forms, respectively. The mouse chordin protein consists of four CRs and is approximately 2 to 2.8

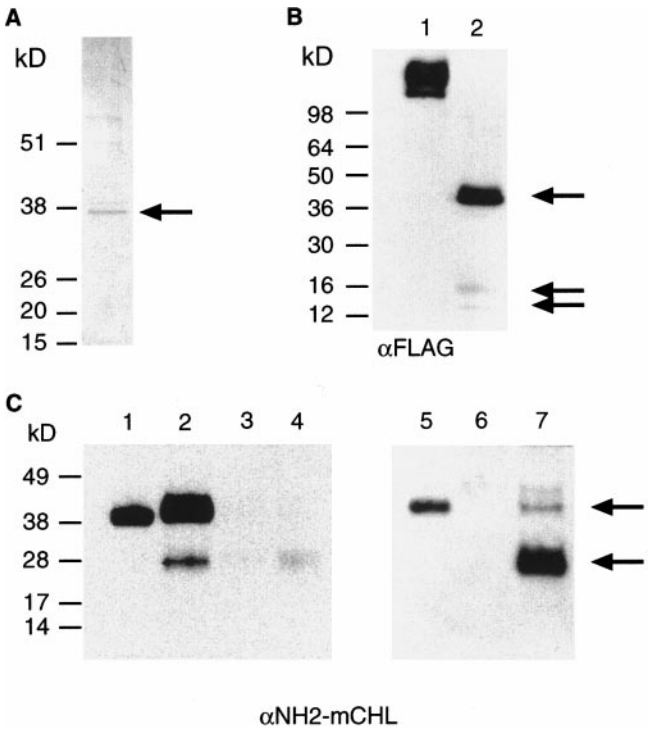

FIG. 3. MCHL(s2) protein. (A) FLAG-tagged CHL(s2) protein purification. The proteins in the peak eluate from anti-FLAG affinity column chromatography (12 μg/ml mCHL(s2)-FLAG determined by Western) were separated by SDS–polyacrylamide gel electrophoresis under reducing conditions and were stained with Coomassie brilliant blue (Sambrook *et al.*, 1989). The arrow indicates the mCHL(s2)-FLAG protein band. This band was excised, and the NH_2-terminal amino acid sequence of the extracted peptide was determined (the vertical arrow in Fig. 1B) to confirm the identity of the band. (B) Western blot analysis of the purified mCHD-FLAG protein (lane 1) and mCHL(s2)-FLAG protein (lane 2). The purified FLAG-tag proteins were visualized with M2 (αFLAG). The arrows indicate the intact mCHL(s2)-FLAG (top) as well as the COOH-terminal portion of the degradation product (lower duplex). (C) Stability of the mCHL(s2) protein. The stable 293 clone for mCHL(s2)-FLAG was plated at 1×10^6 cells/well in a 6-well plate. Twenty-four hours later, the medium was changed to 2 ml each of 293 SFM II (lane 2), DMEM (lane 3), or DMEM with transferrin and insulin (lane 4), and the cultures were incubated further for 48 h. Transient transfection of 293T cells was also performed with pSRαhEPO (lane 6) and pSRαmCHL(s2) (lane 7), and 48-h conditioned media were made with DMEM. All of the culture supernatants were equally concentrated and 40 μl of each was subjected to Western blot analysis with the anti-mCHL antibody (αNH2-mCHL). Lanes 1 and 5 are the purified mCHL(s2)-FLAG proteins. The arrows indicate the intact size of the mCHL(s2) protein (top) as well as the NH_2-terminal portion of the degradation product (bottom).

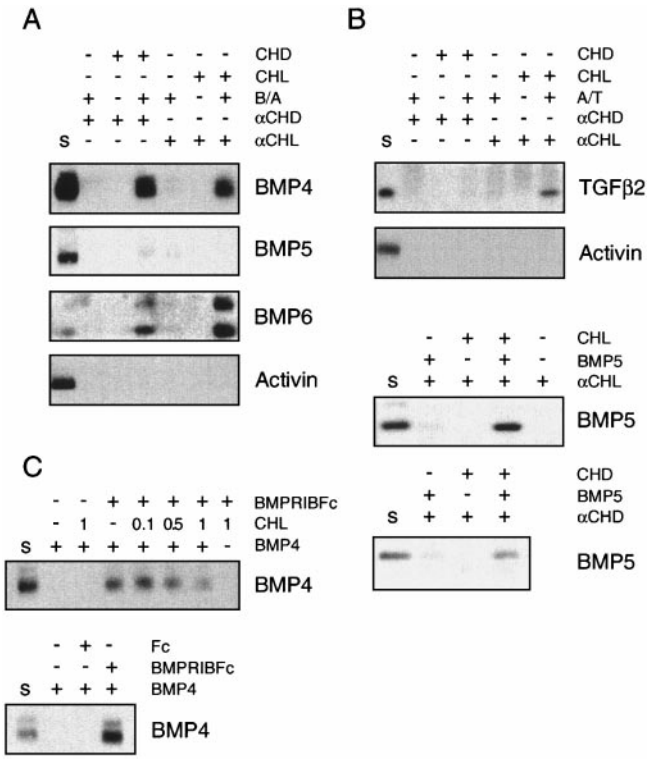

FIG. 4. Direct interaction of mCHL(s2) with BMPs and inhibition of BMP4 binding to the receptor by mCHL(s2). (A) Immunoprecipitation/Western blot analysis under low concentration conditions (see Materials and Methods). MCHL(s2)-FLAG (CHL) and mCHD-FLAG (CHD) were individually mixed with 90 ng of BMP4, 90 ng of BMP5, 0.1 μg of BMP6, or 0.1 μg of activin A and were treated with 1.7 and 3.4 μg of the affinity-purified anti-mCHL (αCHL) and anti-mouse chordin (αCHD) antibodies, respectively. The resulting immunocomplex was precipitated with protein A agarose beads. The lane "S" stands for the standard, on which 20 ng of BMP4, 20 ng of BMP5, 10 ng of BMP6, or 20 ng of activin A was loaded directly. B/A stands for BMP or activin A. (B) Immunoprecipitation/Western blot analysis under the high concentration conditions (see Materials and Methods). Both the mCHL/CHD-FLAG protein and the BMP/activin/TGFβ protein were mixed at a higher concentration. Then, the immunocomplex was formed with anti-mCHL antiserum (αCHL) or anti-mouse chordin antiserum (αCHD) and was precipitated with protein A/G beads. For the standard (S), 40 ng each of TGFβ2, activin A, and BMP5 was loaded directly. A/T stands for activin A or TGFβ2. (C) Inhibition of BMP4 binding to BMPR1B by CHL. (Top panel) mCHL(s2)-FLAG (CHL) was first mixed with BMP4 at various concentrations, as indicated (0.1–1 μg), and then BMPR1BFc was added. The resulting BMPR complex was precipitated, and the bound BMP4 was visualized. (Bottom panel) Binding specificity of BMP4 to the BMPR1B extracellular domain was confirmed. Note that BMP4 was not coprecipitated with human IgG Fc. For the standard (S), 20 ng of BMP4 was loaded directly.

times larger than the mCHL proteins (945 amino acids), as illustrated in Fig. 1A. The CR1 and CR3 of mCHL were most similar to the CR3 of mouse chordin (indicated by black boxes).

The cloning frequency of the different forms of hCHL was not random. For instance, five of five clones isolated from the prostate cDNA library were either hCHL(l3) or hCHL(l4). However, the PCR–based cloning of hCHL from human brain, heart, and prostate cDNAs followed by DNA sequencing revealed that all forms were found in all three tissues (data not shown). Therefore, no tissue-specific expression of any form has been demonstrated. So far, no hCHL cDNA equivalent to mCHL(s2) has been identified, and no mouse equivalents of hCHL(l1), hCHL(l2), and hCHL(l4) have been cloned.

Both Mouse and Human CHL Genes Are Located on the X Chromosome

A partial sequence of the hCHL gene was found in GenBank (Accession No. AL049176). The sequence is derived from the q22.1-23 region of the human X chromosome, and it was found to contain a region from exon 3 to exon 12 of the hCHL gene. The mCHL gene was mapped by FISH using a BAC clone DNA with a chromosomal DNA segment containing CHL exons as a probe. The mCHL gene was located at a position 89% of the distance from the heterochromatic–euchromatic boundary to the telomere of the X chromosome, which corresponds to band XF3. Therefore, both the human and mouse CHL genes are located on the X chromosome.

The Multiple Forms of the CHL cDNAs Were Probably Created by Alternative Splicing and Alternative Transcriptional Termination

It was evident from the AL049176 genomic DNA sequence that hCHL(l2) could be formed by the use of an alternative splice acceptor for intron 4 and that hCHL(l3) was likely to be generated by the use of an alternative splice donor for intron 9 (Fig. 1C). The mCHL(s2) protein ended 10 amino acids (GALAGGPAFG) after the GKKAK sequence (Fig. 1B). It was found from the human genomic sequence that an almost identical amino acid stretch, GALVGGPAFG, could be added after GKKAK if no splicing of intron 9 occurred. This would also result in an almost identical size as the mCHL(s2) protein (333 and 332 amino acids for hCHL(s1) and for hCHL(s2), respectively). The 3′-UTR of the mCHL(s2) cDNA was homologous to intron 9 of the hCHL gene, but not to the hCHL(l) 3′-UTR in exon 12 (data not shown). These observations suggest that the CHL(s) cDNAs were probably derived from the CHL transcripts that prematurely terminated within intron 9 or from the splice variants retaining intron 9. On the other hand, the 3′-UTR of the mCHL(l3) cDNA was homologous to the hCHL(l) 3′-UTR, suggesting that the mCHL(l3) transcript stops at a similar site as the hCHL(l) transcripts. Thus, the CHL variants were probably generated by alternative splicing and/or alternative transcriptional termination.

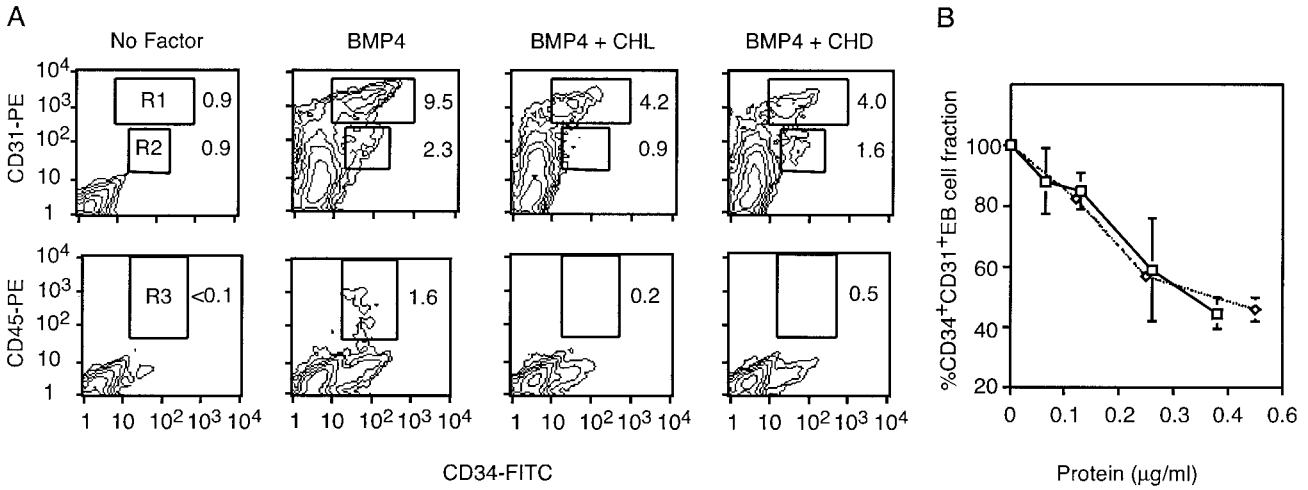

FIG. 5. Inhibitory effects of mCHL(s2) and mouse chordin proteins on the BMP4-dependent differentiation of ES cells *in vitro*. (A) Effects on the generation of the $CD34^+CD31^{hi}$ lymphohematopoietic progenitor cell fraction (R1), the $CD34^+CD31^{lo}$ erythromyeloid progenitor cell fraction (R2), and the $CD45^+$ myelomonocytic cell fraction (R3). Seven-day-old embryoid bodies (EBs) generated without a factor (No factor), with BMP4 (BMP4), with BMP4+0.4 μg/ml mCHL(s2)-FLAG (BMP4+CHL), and with BMP4+0.5 μg/ml mCHD-FLAG (BMP4+CHD) were harvested and analyzed for CD34, CD31, and CD45 protein expression. Numbers indicate percentages of total EB cells. (B) Dose-dependent inhibition of the BMP4-dependent generation of the $CD34^+$ $CD31^+$ progenitor cell fraction. ES cells were differentiated in the presence of BMP4 and various concentrations of mCHL(s2)-FLAG or mCHD-FLAG protein. The $CD34^+CD31^+$ EB cell populations (R1+R2) were individually normalized in each experiment so that 100% corresponds to the $CD34^+CD31^+$ EB cell fraction obtained without mCHL-FLAG and mCHD-FLAG. Values obtained from two to three independent experiments were averaged and plotted according to the concentration of mCHL(s2)-FLAG (□) and mCHD-FLAG protein (◇) added. The vertical bars are the standard deviation.

CHL Induced a Secondary Axis in the Xenopus Embryo: Evidence for in Vivo Interaction with BMP

Chordin is known to dorsalize the gastrulating *Xenopus* embryo by inhibiting the activity of BMP4. Therefore, the effects of the CHLs on *Xenopus* embryo development were examined (Fig. 2 and Table 1). When 10–30 pg RNA was injected per blastomere, the axis duplication rates for mCHL(s2) and for mCHL(s2)-FLAG ranged from 79 to 87%, whereas the rate for the uninjected control embryos and the EF1 RNA-injected embryos was 0% (Table 1). As a positive control, experiments were also performed with the mCHD-FLAG RNA, and an axis duplication rate similar to that of mCHL(s2) was obtained (Table 1). Thus, mCHL(s2), with or without a FLAG tag at the COOH terminus, was active in antagonizing the endogenous ventralizing factor (presumably BMP4). The hCHL constructs, including long forms (l1 and l2) and short forms (s1 and s2), displayed essentially the same effect as mCHL(s2), although the maximum tolerable amount of RNA (1 ng) was required. This result indicates that all forms of CHL tested were active in antagonizing the *Xenopus* ventralizing factor and suggests that the mouse CHL seemed to be more active in *Xenopus* embryos than the human CHLs.

The mCHL(s2) Protein Is Potentially Cleaved between CR2 and CR3

Further protein analyses were carried out with mCHL(s2). As shown in Figs. 3A and 3B, a single step of affinity purification resulted in FLAG-tagged proteins of the expected sizes (the apparent size of mCHL(s2) was approximately 38 kD). During the purification, it was noticed that the expression levels as well as the integrity of mCHL(s2)-FLAG in serum-free conditioned media depended entirely on the type of medium used. For instance, DMEM with or without insulin and transferrin yielded only a very low level of the protein, which was mostly degraded (Fig. 3C). Other media, such as s-MEM and IMDM, also gave similar results (data not shown). The degradation product that cross-reacted with the anti-NH_2-terminal peptide antibody was approximately 28 kDa in size (Fig. 3C), and those that cross-reacted with the anti-FLAG antibody were 14 to 16 kDa (Fig. 3B). Based on the sizes of these degradation products, the predicted degradation sites were mapped between CR2 and CR3. In contrast, 293 SFM II protected the mCHL(s2)-FLAG protein from degradation and gave reasonable expression levels. Nevertheless, the CHL protein seemed to be unstable and susceptible to protease attack.

Direct Interaction of mCHL(s2) with BMPs and Inhibition of BMP Binding to the Receptor by mCHL(s2)

The direct interaction of the *Xenopus* chordin protein with human BMP4 has been demonstrated (Piccolo *et al.*, 1996). Similar experiments were performed using the mouse chordin and mouse CHL proteins. As shown in Figs. 4A and 4B, both the mCHD-FLAG and mCHL(s2)-FLAG proteins co-immunoprecipitated with BMP4, BMP5, and BMP6. However, under the low concentration condition (Fig. 4A), BMP5 showed no sign of interaction with mCHL(s2)-FLAG and a very weak interaction with mCHD-FLAG. On the other hand, BMP6 gave significantly weaker signals for both proteins compared with the high concentration condition. These observations suggest that both chordin and CHL might have weaker affinities with BMP5 and BMP6 than with BMP4. Activin A, another TGFβ superfamily member, showed no sign of interaction with chordin and CHL under either set of conditions. BMP2 and BMP4 form a separate subfamily from BMP5, BMP6, and BMP7 (Celeste *et al.*, 1990). Thus, both the chordin and CHL proteins may be pan-BMP binding proteins. Interestingly, mCHL(s2)-FLAG, but not mCHD-FLAG, interacted with TGFβ1 (data not shown) and TGFβ2 (Fig. 4B) under the high concentration condition.

Chordin prevents BMP action by inhibiting the interactions of BMPs with their receptors. Therefore, we determined whether CHL functioned in a similar fashion. The extracellular domain of the BMP receptor 1B fused to the Fc portion of human IgG (BMPR1BFc) was mixed with BMP4 and was precipitated with protein A beads. As shown in Fig. 4C, without the mCHL(s2)-FLAG protein, BMP4 was coprecipitated with BMPR1BFc but not with Fc, indicating that BMP4 bound specifically to the BMPR1B extracellular domain. With increasing amounts of mCHL(s2)-FLAG added, however, the BMP4 signal became weaker. At concentrations of 0.5 μg/ml or higher, the reduction was especially evident. This result suggests that, similar to chordin, CHL may also prevent BMP4 from binding to the receptor.

MCHL(s2) Inhibits BMP4 Action in Vitro

Complex formation with chordin is known to inhibit BMP4 function. Judging from the similar axis duplication activity to chordin, CHL would also inhibit BMP4 action directly. We have demonstrated previously that the generation of $CD34^+$ $CD31^{hi}$ lymphohematopoietic progenitor cells, $CD34^+$ $CD31^{lo}$ erythromyeloid progenitor cells, and $CD45^+$ myelomonocytic cells is dependent on the presence of 0.15 to 2 ng/ml of BMP4 during the differentiation of mouse ES cells (Nakayama *et al.*, 2000). A BMP4 concentration of 0.6 ng/ml resulted in an approximately half-maximal level (data not shown). When affinity-purified mCHL(s2)-FLAG and mCHD-FLAG proteins were each added, at 10 to 500 ng/ml per assay, the $CD34^+$ $CD31^{hi}$, $CD34^+$ $CD31^{lo}$, and $CD45^+$ cell populations were significantly reduced (Fig. 5A), and this inhibition was dose-dependent (Fig. 5B). These results suggest that the FLAG-tagged CHL and chordin proteins were each able to inhibit the action of BMP4 *in vitro.*

Localization of CHL mRNA Expression

A Northern blot analysis indicated that CHL and chordin were differentially expressed over time during mouse embryogenesis (Fig. 6A). The E7 mouse embryo as a whole expressed chordin mRNA but not CHL mRNA, whereas the pattern was reversed in embryos later than E11. In the adult mouse (Fig. 6B), distinct patterns of expression were maintained. CHL transcripts 4 kb in length were present in brain, lung, kidney, and testis. However, liver expression was consistently very low. On the contrary, the chordin mRNA was detected mainly in the liver and brain. In humans, the chordin mRNA was detected predominantly in the liver (data not shown).

It is worth noting that no transcript significantly longer than 4 kb was observed on the Northern blots. Furthermore, the specific probe for the mCHL(s) mRNA (intron 9 probe) detected only transcripts with a similar size (approximately 4 kb) in mouse embryos and adult tissues. The intron 9 of the human CHL gene is approximately 6.9 kb in length. Assuming that the intron 9 of the mouse CHL gene has a similar size, these observations support the idea that the mCHL(s) mRNA might be generated by premature termination (Fig. 1C).

CHL mRNA Expression during Skeletogenesis

An *in situ* hybridization analysis revealed CHL expression beginning around embryonic day 9.5 and persisting in a wide range of adult stromal and connective tissue cell types of mesenchymal origin. No CHL signal was detected in the sections examined at E8.5. At E9.5, the signal was just barely detectable over the somites but not the limb bud (data not shown). At E10.5, strong signals were seen over the dermatome portion of the somites and diffusely over the limb bud mesenchyme (Figs. 7A–7D). In the E11.5 limb (Figs. 7G and 7H) and elsewhere throughout the developing skeleton (data not shown), the CHL mRNA was present over areas of mesenchymal cells concurrent with the formation of precartilaginous mesenchymal condensations. At E12.5, this included the cephalic mesenchyme in areas where the basioccipital and exoccipital bones form, over mesenchymal cells in the mandible, and adjacent to the dorsal root ganglia in areas where vertebrae would form (data not shown). At E13.5, strong CHL signals were detectable over the hypertrophic chondrocytes in limb bones (Figs. 7I and 7J), clavicle, and sternum, as well as in the perichondrial mesenchymal cells adjacent to the developing joints. Strong CHL expression continued in the hypertrophic chondrocytes within the developing bones (E15.5, Figs. 7E, 7F, 7K, and 7L) and began to decline in the perichondrial mesenchymal cells, a pattern that contrasts with that of chordin (Fig. 7M), which was

strikingly absent in the cartilage elements. By E18.5 and through to the adult, the skeletal expression of CHL was present at diminished levels and was restricted to the hypertrophic chondrocytes at the epiphyseal growth plate, scattered cells in the bone marrow, which appeared to be a population of bone marrow stromal cells (Figs. 7N, 7O, 8A, and 8B), and at barely detectable levels in the articular chondrocytes at the joint surfaces.

Nonskeletal Expression of CHL

CHL was also expressed in a range of nonskeletal mesenchymal cell types. Expressions in subdermal fusiform stromal cells, connective tissue cells of the epimysium and perimysium surrounding bundles of skeletal muscle, a layer of fibroblast/connective tissue cells dividing the submucosa and muscularis of the gastrointestinal tract (Figs 8C and 8D), and perivascular cells were all detectable embryonically and persisted into adulthood. A strong and striking pattern of adult CHL expression was present in the outer medulla and medullary rays of the kidney (Fig. 8E). The CHL-positive cells formed segments of proximal and distal tubules, derived from the nephrogenic mesenchyme (Fig. 8F). Additional sites of adult CHL expression included trabecular connective tissue cells in the lymph nodes, perivascular cells in the lung, myofibroblasts in the uterus, and stromal cells in white adipose tissue (data not shown).

In addition to these mesenchymal cell types, the signal was detected at E10.5 in the differentiating fields of the ventral telencephalon and the dorsal rhombencephalon, which are destined to become the olfactory bulb and the cerebellum, respectively. Other parts of the developing nervous system lacked CHL expression. The CHL expression in these regions persisted through embryonic development, and adult cerebellar Purkinje cells (Figs. 8G and 8H), olfactory bulb neurons, and cerebral cortical neurons (and glia-like cells) continued to express CHL.

Thus, the CHL gene was expressed preferentially in cell types originating from the embryonic mesenchyme. The only nonmesenchymal cell lineage expressing the CHL mRNA was the neuron.

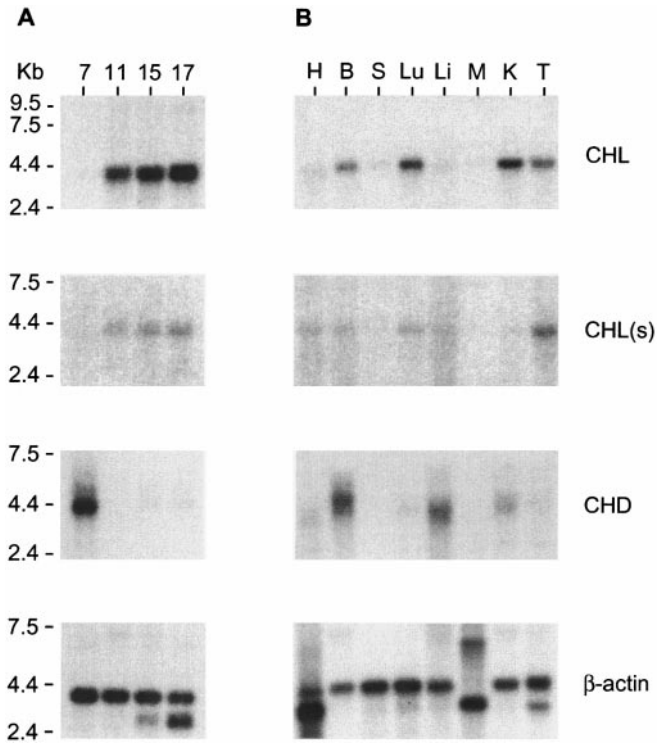

FIG. 6. Differential expression of the CHL gene and the chordin gene. Northern blot analyses were performed using Clontech blots. The blots were first probed with a DNA containing the mCHL(s2) ORF (CHL) and then were reprobed with the mouse chordin cDNA (CHD) and finally with the human β-actin fragment (β-actin). Three different batches of blots were used. All gave essentially the same results. A separate batch of RNA blot was probed with the intron 9 probe to detect the mCHL(s)-specific transcript (CHL(s)). The pattern of expression of the β-actin mRNA (not shown) was indistinguishable from that shown here. (A) Mouse embryo blot made with E7 (7), E11 (11), E15 (15), and E17 (17) embryo-derived RNA. (B) Mouse adult tissue blot made with heart (H), brain (B), spleen (S), lung (Lu), liver (Li), skeletal muscle (M), kidney (K), and testis (T) RNAs.

FIG. 7. CHL mRNA expression during embryogenesis. *In situ* hybridization for CHL in normal mouse embryos, depicted in paired brightfield (left) and darkfield (right) panels. (A, B) Sagittal section through an E10.5 mouse demonstrates CHL expression in the somites and a diffuse signal in the limb bud. (C, D) Higher magnification of the boxed area in A shows the CHL signal in the dermatome portion of the somites at E10.5. (E, F) Transverse section through the thoracic region at E15.5. Arrowheads indicate the expression of CHL in the hypertrophic chondrocytes in the neural arch, radius, metacarpal, and phalangeal bones. The signal is also present in areas of condensed mesenchyme adjacent to the developing bones and in subcutaneous stromal cells. (G–O) Higher magnification views of the forelimb of E11.5, E13.5, E15.5, and E18.5 embryos. Arrowheads indicate CHL-positive hypertrophic chondrocytes in the growth plate regions of the developing radius. (G, H) At E11.5, the signal is present over areas of mesenchymal cells as precartilaginous mesenchymal condensations begin to form. (I, J) At E13.5, CHL expression is detectable over the hypertrophic chondrocytes in the radius (arrowhead) and in the perichondrial mesenchymal cells adjacent to the elbow and wrist joints. (K, L) At E15.5, CHL expression in the limb is most notable in the hypertrophic chondrocytes of the radius, tarsals, metatarsals, and phalanges (arrowheads). (M) *In situ* hybridization with a chordin probe in an E15.5 section adjacent to K demonstrates a conspicuous lack of chordin expression in cartilage elements. (N, O) At E18.5, CHL expression in bone is restricted to hypertrophic chondrocytes at the epiphyseal growth plates. Abbreviations used: lb, limb bud; h, heart; hu, humerus; ra, radius; eso, esophagus; sp, spinal cord; na, neural arch; gut, intestine; d, digit; li, liver; lu, lung. Scale bars are indicated on the brightfield panels.

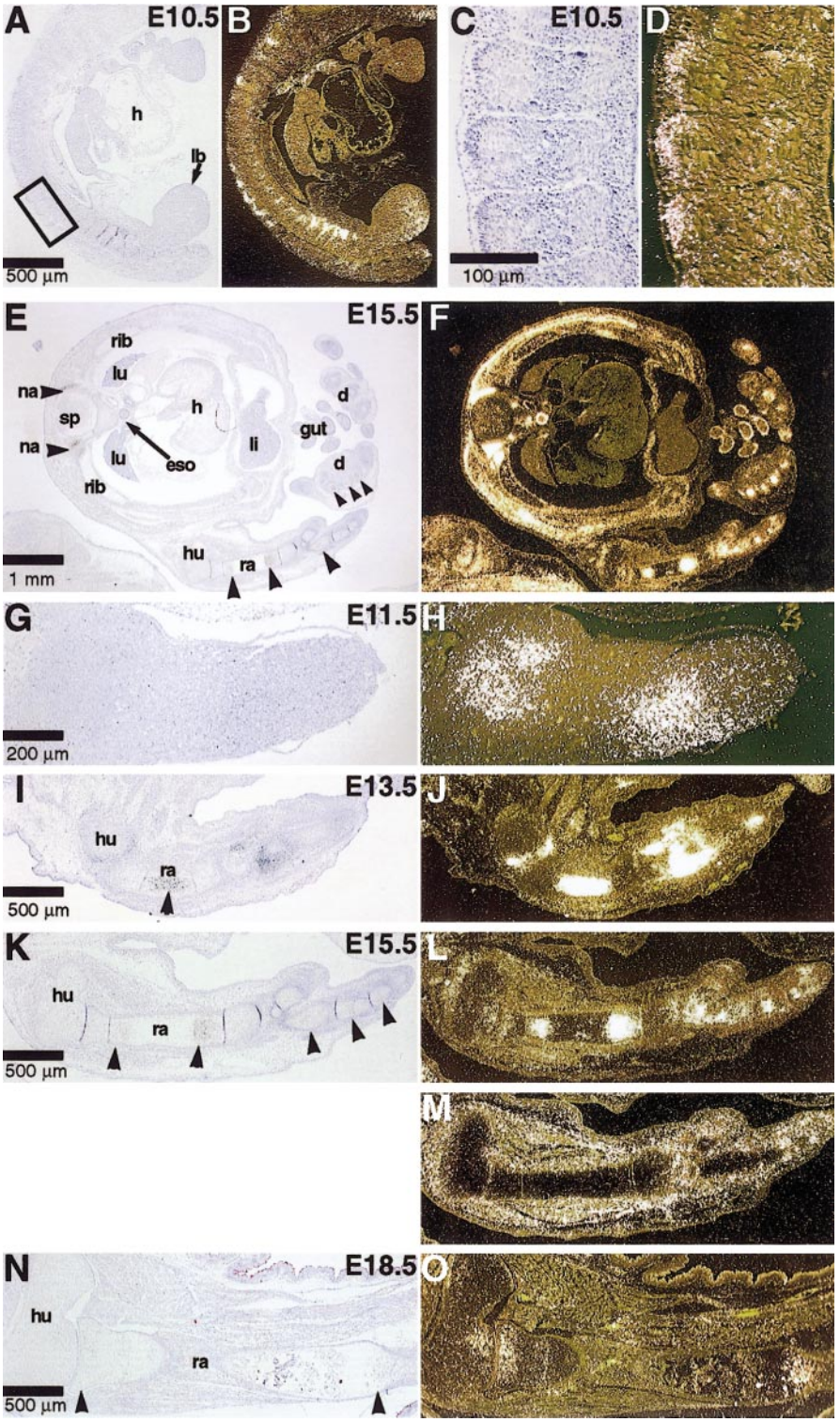

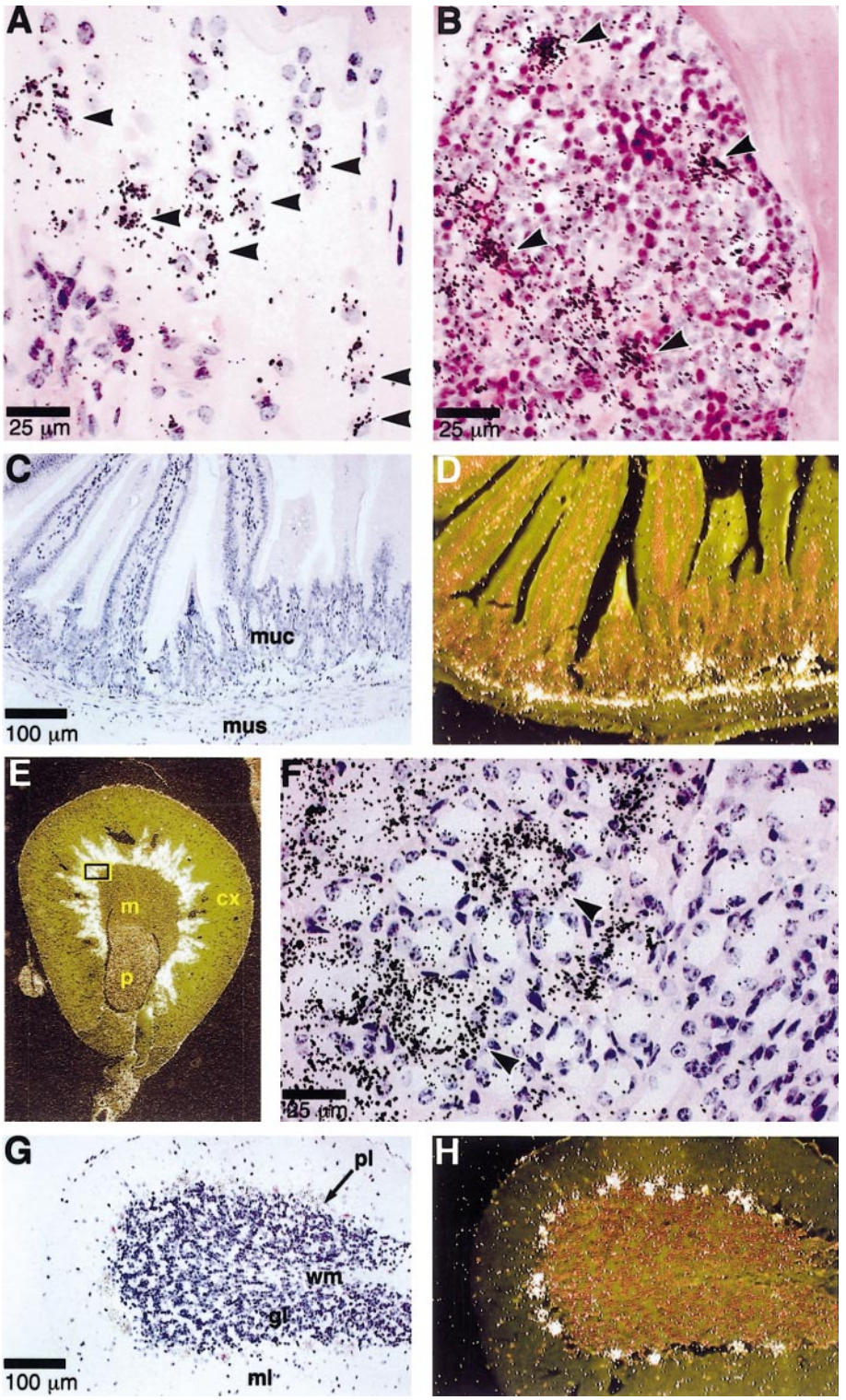

FIG. 8. Expression of CHL mRNA in adult mouse tissues. *In situ* hybridization for CHL in normal adult mouse tissue. (A) Longitudinal section through the epiphyseal growth plate region of the adult femur. Arrowheads indicate expression of CHL mRNA in hypertrophic chondrocytes. (B) CHL-positive cells in the bone marrow (arrowheads) appear to be a population of bone marrow stromal cells. (C, D) Paired bright- and darkfield images of a cross section through the duodenum, showing CHL mRNA expression in a layer of stromal/connective tissue cells between the submucosa and muscularis. (E, F) Transverse section through a normal adult mouse kidney, showing expression of CHL mRNA primarily in the region of the outer medulla and medullary rays. The boxed area in E is shown at a higher magnification in F, where the signal appears to be localized in segments of the thick ascending tubules (arrowheads). (G, H) CHL mRNA is expressed in the Purkinje cell layer of the cerebellum. Abbreviations used: muc, submucosa; mus, muscularis; cx, cortex; m, medulla; p, papilla; gl, granule cells; wm, white matter; pl, Purkinje cell layer; ml, molecular layer. Scale bars are indicated.

DISCUSSION

We have demonstrated that a novel X-linked chordin-like gene, CHL, encodes a protein that directly interacts with BMPs and inhibits their actions *in vitro* as well as *in vivo*. The expression analysis suggests a possible role of CHL during skeletogenesis as well as in several other organogenic processes. This is the first demonstration that a chordin-type BMP inhibitor forms a gene family in mammals.

Structure and Function of CHL

Based on the Gap analysis (Genetics Computer Group), the overall amino acid sequence similarity between the mouse chordin and mCHL(s2) was 28%, and the nucleic acid homology of the ORF was 37%. Only the CR units showed statistically significant homology. Therefore, the sequence homology was not sufficient to imply functional similarities between chordin and CHL. However, when injected into early *Xenopus* embryos, the CHL RNA showed a clear axis duplication activity similar to that of mouse chordin RNA (Fig. 2). In fact, recombinant mCHL(s2) protein and mouse chordin protein were able to interact directly with the three BMPs tested (Fig. 4). Both proteins also inhibited BMP function *in vitro* when added to the serum-free differentiation culture of ES cells, which leads to the generation of lymphohematopoietic progenitor cells in a BMP4-dependent manner (Fig. 5 and Nakayama *et al.*, 2000). Furthermore, the inhibition of BMP action by the mCHL(s2) protein seemed to be achieved by preventing BMP4 from interacting with the BMP receptor (Fig. 4C). These results suggest that CHL is not only structurally related to but also functionally similar to chordin.

One difference in the activities of CHL and chordin was the target specificity. MCHL(s2) showed weak but sufficient binding capability to be coprecipitated with TGFβ1 (data not shown) and TGFβ2 (Fig. 4B) when the high concentration conditions were used. In contrast, mouse chordin did not show any sign of interaction with them, consistent with the properties of *Xenopus* chordin (Piccolo *et al.*, 1996). However, we still have not succeeded in determining whether the interaction with CHL inhibits TGFβ function.

CHL was present in multiple forms in both mouse and human (Fig. 1). As in the case of chordin, these variations could change some of the CHL activities (Yu *et al.*, 2000). However, given that the two long forms, l1 and l2, and the two short forms, s1 and s2, induced a secondary axis in the *Xenopus* embryo (Table 1), all forms are likely to share the BMP-antagonizing activity. Interestingly, all of the variations are located outside the CRs: $E^{95/96}$ directly follows CR1, the GKKAK is immediately after CR3, and the short form contains an altered COOH-terminal sequence after the GKKAK (Fig. 1B). Since the CRs are the binding sites for BMPs (Larrain *et al.*, 2000), these variations may not affect the CHL's binding specificity to BMPs. On the other hand, they may affect the stability and/or integrity of the protein. In this regard, it is worth noting that the axis duplication rates obtained with the long forms of hCHL fluctuated significantly, even when 1 ng of RNA was injected per blastomere, while the short forms of hCHL gave more consistent and higher values, suggesting that the short forms might be more stable and/or active than the long forms of CHL.

The mCHL(s2) protein was unstable and readily degraded in conditioned media (Fig. 3C). This was also the case for the hCHL(l1) protein (data not shown). Therefore, CHL protein instability does not seem to be specific for either the mouse protein or the short form. It is known that BMP1/Tolloid inactivates chordin (Piccolo *et al.*, 1997; Scott *et al.*, 1999). Interestingly, CHL contained potential BMP1 target sites between CR2 and CR3, the area consistent with our estimated degradation sites (Fig. 1). Therefore, CHL could be under the BMP1-dependent control mechanism. There were also several potential cleavage sites (K/R-(X)n-K/R, $n = 0$, 2, 4, or 6) for proprotein convertase between CR2 and CR3 (reviewed in Seidah and Chretien, 1999). Therefore, what appeared to be degradation products could be mature forms of CHL. These degraded/processed products of CHL may show very weak inhibitory activity (Larrain *et al.*, 2000) and/or possess altered target specificity (Yu *et al.*, 2000), as in the case of chordin. Supporting the former, the mCHL(s2) preparation, made through transient transfection of 293T cells, which was mostly composed of degraded/processed products (Fig. 3C), was not active in suppressing BMP4 activity during ES cell differentiation (data not shown). Thus, if the degraded/processed forms are the functional forms *in vivo*, then the biological role of CHL could be agonistic instead of antagonistic to BMP action.

Further biochemical characterizations of CHL as well as the CHL variants and genetic analysis of the CHL gene would provide definitive answers to these questions.

Biological Implications of CHL

The CHL transcript was first detected in the somites of the E9.5 mouse embryo, and at E10.5, strong signals were observed in the dermatome and limb bud mesenchymes (Figs. 7A–7D). Consistently, the developing skeletal structure, including limb bones, clavicle, calvaria, vertebra, and rib (ex. at E15.5, Figs. 7E and 7F), was one of the major CHL expression sites during embryogenesis. During the limb bone formation, the CHL expression was first detected in the precartilaginous mesenchymal condensation of the limb bud (Figs. 7G and 7H) and later was restricted to the hypertrophic chondrocytes in the epiphyseal growth regions, and its expression levels progressively diminished as the embryo developed (Figs. 7I–7O and 8A). On the contrary, the chordin-expressing sites in the forelimb did not overlap with the CHL-expressing areas (they were like a mirror image), suggesting that chordin and CHL would have different and/or non-overlapping biological roles during limb formation (Figs. 7K–7M). This observation supports

the previous finding that in the E15.5 hindlimb, the chordin transcript is detected throughout the limb mesenchyme, with particularly high levels of expression overlying the perichondrium of the ossifying cartilage of the femur as well as that of the cartilage primordia of the tarsals, metatarsals, and phalanges (Scott *et al.*, 1999, 2000). Similarly, Gremlin, another BMP binding inhibitor family, is expressed in the nonchondrogenic region of the limb bud and later in the interdigital mesenchyme and the differentiating perichondrium (Merino *et al.*, 1999). However, the expression sites of the CHL mRNA in the developing limb overlapped somewhat with those of noggin mRNA, including the mesenchymal condensations in the limb bud and the chondrocytes of the developing limb bone (Brunet *et al.*, 1998; Capdevila and Johnson, 1998; Merino *et al.*, 1998; Nifuji and Noda, 1999; Pathi *et al.*, 1999). Nevertheless, since BMPs are expressed in the limb cartilage, the sternum, and the rib during mouse embryogenesis (Solloway *et al.*, 1998; and reviewed in Wozney *et al.*, 1993) and are implicated in many stages of bone formation (reviewed in Karsenty, 1998), these results support the hypothesis that CHL may participate in regulating BMP action during skeletogenesis, and the biological role of CHL may be shared in part by noggin.

On the other hand, the expression of CHL mRNA in nonskeletal mesenchymal cells in the embryo, such as subdermal mesenchymes and gut mesenchymes (Figs. 7E and 7F), seemed to continue into many adult connective tissue cell types. For example, in the stomach, the intestine, and the colon, the expression was localized specifically on a layer of fibroblasts/connective tissue cells that divided the submucosa and muscularis (Figs. 8C and 8D). In contrast, the chordin signal was detected weakly over the connective tissue cells in the muscularis of the gastrointestinal tract and was never restricted to a single layer (data not shown). During the gastrointestinal development of the chicken, BMP4 is induced in the non-smooth muscle mesenchyme around the endodermal epithelium, which later differentiates into the submucosa, and inhibits the differentiation of smooth muscle and enteric neurons in the muscularis (Smith *et al.*, 2000; Sukegawa *et al.*, 2000). In this respect, the layer of CHL-expressing cells may serve as a wall that prevents the migration of active BMPs into the muscularis. Furthermore, the strong CHL signal in the tubules of the kidney outer medulla (Figs. 8E and 8F) suggests that CHL may also be involved in mesenchymal cell differentiation during nephrogenesis, especially because BMP is required for the nephrogenic mesenchyme to grow and survive, but is inhibitory for tubulogenesis (Dudley *et al.*, 1999). In contrast, the chordin signal was observed only in a layer of connective tissue/fibroblast-like cells beneath the urothelium lining, the portion of the renal pelvis that connects to the ureter (data not shown). Thus, CHL and chordin are also differentially expressed in the kidney.

CHL mRNA expression in mesenchymal cell lineages is consistent with our isolation of the cDNA from the preadipocytic stromal cell line OP9. In fact, in both the vertebrae (data not shown) and the adult femur (Fig. 8B), the *in situ* hybridization signal was detected over the nonhematopoietic cell types in the marrow space. The chordin signal in the bone marrow was too weak to detect (data not shown). Whether CHL and BMPs have any role in hematopoiesis remains to be determined. In this respect, it is worth mentioning that the CHL mRNA expression in bone marrow stromal cell lines has some correlation with their ability to support long-term *in vitro* hematopoiesis (data not shown).

The expression of CHL in restricted areas of the developing brain suggests a possible role of CHL in the regulation of BMP activity during the generation of specific neurons: olfactory bulb neurons and Purkinje cells. Supporting this hypothesis, BMPs are expressed on the Purkinje cell layer (Nakashima *et al.*, 1999; Zhao *et al.*, 1999), and the involvement of BMPs in cerebellar granule neuron genesis has been demonstrated recently (Alder *et al.*, 1999). Interestingly, there were also differences between the expression domains of chordin and those of CHL in the adult brain. For instance, a strong chordin signal was detected over the hippocampus (including the dentate gyrus), where the CHL signal was absent (N. Nakayama, unpublished results; Scott *et al.*, 2000). Furthermore, in the cerebellum, the chordin transcript was detected over granule cells, but not on Purkinje cells (N. Nakayama, unpublished results; Scott *et al.*, 2000).

In conclusion, a large body of evidence has suggested that the function of BMP is regulated by a variety of binding proteins in the extracellular space. In this respect, the identification of CHL provides additional support for the idea that this regulatory mechanism is widely employed for BMPs and that individual BMP binding proteins are responsible for eliciting the distinct biological roles of the BMPs. Some questions remain: does CHL play an indispensable role at any of the expression sites and is the spatiotemporal control of CHL gene expression critical? However, the results that CHL inhibited BMP action, that the main and initial expression sites during embryogenesis were the developing skeleton, and that it was differentially expressed from chordin in many areas have prompted us to speculate that there may be a biological process in which CHL plays an essential role and that it would include skeletogenesis. Thus, the present demonstration may also provide further insights into how BMP actions are regulated spatially and temporarily during organogenesis.

ACKNOWLEDGMENTS

First we acknowledge the scientists and the technicians in the Genomics groups and the Department of Computational Biology for constructing the nucleotide sequence databases and for help with their analysis. We also acknowledge the Amgen CORPS group for coordinating the middle-scale CHL protein purification. We greatly appreciate the contributions of J. Hui and M. Haniu in determining the NH_2-terminal amino acid sequences of the mature CHL and chordin proteins. Finally, we give warm thanks to S. Wooden for providing plasmids, to J. Li, S. Simonet, and W. Boyle for sharing information and interesting discussions, to S. Simonet

for critical reading of the manuscript, and to S. Simonet and W. Boyle for support and encouragement. R.N. and T.Y. are supported by Japan Amgen, K.K.

REFERENCES

Adams, M. D., Kelley, J. M., Gocayne, J. D., Dubnick, M., Polymeropoulos, M. H., Xiao, H., Merril, C. R., Wu, A., Olde, B., Moreno, R. F., Kerlavage, A. R., McCombie, W. R., and Venter, J. C. (1991). Complementary DNA sequencing: Expressed sequence tags and human genome project. *Science* **252,** 1651–1656.

Adra, C. N., Boer, P. H., and McBurney, M. W. (1987). Cloning and expression of the mouse pgk-1 gene and the nucleotide sequence of its promoter. *Gene* **60,** 65–74.

Alder, J., Lee, K. J., Jessell, T. M., and Hatten, M. E. (1999). Generation of cerebellar granule neurons *in vivo* by transplantation of BMP-treated neural progenitor cells. *Nat. Neurosci.* **2,** 535–540.

Bachiller, D., Klingensmith, J., Kemp, C., Belo, J. A., Anderson, R. M., May, S. R., McMahon, J. A., McMahon, A. P., Harland, R. M., Rossant, J., and De Robertis, E. M. (2000). The organizer factors Chordin and Noggin are required for mouse forebrain development. *Nature* **403,** 658–661.

Belo, J. A., Bouwmeester, T., Leyns, L., Kertesz, N., Gallo, M., Follettie, M., and De Robertis, E. M. (1997). Cerberus-like is a secreted factor with neutralizing activity expressed in the anterior primitive endoderm of the mouse gastrula. *Mech. Dev.* **68,** 45–57.

Biben, C., Stanley, E., Fabri, L., Kotecha, S., Rhinn, M., Drinkwater, C., Lah, M., Wang, C. C., Nash, A., Hilton, D., Ang, S. L., Mohun, T., and Harvey, R. P. (1998). Murine cerberus homologue mCer-1: A candidate anterior patterning molecule. *Dev. Biol.* **194,** 135–151. doi: 10.1006/dbio/1997.8812.

Bouwmeester, T., Kim, S., Sasai, Y., Lu, B., and De Robertis, E. M. (1996). Cerberus is a head-inducing secreted factor expressed in the anterior endoderm of Spemann's organizer. *Nature* **382,** 595–601.

Brunet, L. J., McMahon, J. A., McMahon, A. P., and Harland, R. M. (1998). Noggin, cartilage morphogenesis, and joint formation in the mammalian skeleton. *Science* **280,** 1455–1457.

Capdevila, J., and Johnson, R. L. (1998). Endogenous and ectopic expression of noggin suggests a conserved mechanism for regulation of BMP function during limb and somite patterning. *Dev. Biol.* **197,** 205–217. doi: 10.1006/dbio/1997.8824.

Celeste, A. J., Iannazzi, J. A., Taylor, R. C., Hewick, R. M., Rosen, V., Wang, E. A., and Wozney, J. M. (1990). Identification of transforming growth factor beta family members present in bone-inductive protein purified from bovine bone. *Proc. Natl. Acad. Sci. USA* **87,** 9843–9847.

Dale, L., and Wardle, F. C. (1999). A gradient of BMP activity specifies dorsal-ventral fates in early *Xenopus* embryos. *Semin. Cell Dev. Biol.* **10,** 319–326. doi: 10.1006/scdb/1999.0308.

Dudley, A. T., Godin, R. E., and Robertson, E. J. (1999). Interaction between FGF and BMP signaling pathways regulates development of metanephric mesenchyme. *Genes Dev.* **13,** 1601–1613.

Francois, V., Solloway, M., O'Neill, J. W., Emery, J., and Bier, E. (1994). Dorsal-ventral patterning of the *Drosophila* embryo depends on a putative negative growth factor encoded by the short gastrulation gene. *Genes Dev.* **8,** 2602–2616.

Fuerthauer, M., Thisse, B., and Thisse, C. (1999). Three different noggin genes antagonize the activity of bone morphogenetic proteins in the zebrafish embryo. *Dev. Biol.* **214,** 181–196. doi: 10.1006/dbio/1999.9401.

Harland, R., and Gerhart, J. (1997). Formation and function of Spemann's organizer. *Annu. Rev. Cell Dev. Biol.* **13,** 611–667.

Harlow, E., and Lane, D. (1988). "Antibodies: A Laboratory Manual." Cold Spring Harbor Laboratory Press, Cold Spring Harbor, NY.

Hogan, B. L. (1996). Bone morphogenetic proteins: Multifunctional regulators of vertebrate development. *Genes Dev.* **10,** 1580–1594.

Hsu, D. R., Economides, A. N., Wang, X., Eimon, P. M., and Harland, R. M. (1998). The *Xenopus* dorsalizing factor Gremlin identifies a novel family of secreted proteins that antagonize BMP activities. *Mol. Cell* **1,** 673–683.

Jacobs, K. A., Collins-Racie, L. A., Colbert, M., Duckett, M., Golden-Fleet, M., Kelleher, K., Kriz, R., LaVallie, E. R., Merberg, D., Spaulding, V., Stover, J., Williamson, M. J., and McCoy, J. M. (1997). A genetic selection for isolating cDNAs encoding secreted proteins. *Gene* **198,** 289–296.

Karsenty, G. (1998). Genetics of skeletogenesis. *Dev. Genet.* **22,** 301–313.

Klein, R. D., Gu, Q., Goddard, A., and Rosenthal, A. (1996). Selection for genes encoding secreted proteins and receptors. *Proc. Natl. Acad. Sci. USA* **93,** 7108–7113.

Larrain, J., Bachiller, D., Lu, B., Agius, E., Piccolo, S., and De Robertis, E. M. (2000). BMP-binding modules in chordin: A model for signalling regulation in the extracellular space. *Development* **127,** 821–830.

Lemaire, P., Garrett, N., and Gurdon, J. B. (1995). Expression cloning of Siamois, a *Xenopus* homeobox gene expressed in dorsal-vegetal cells of blastulae and able to induce a complete secondary axis. *Cell* **81,** 85–94.

Matsui, M., Mizusek, K., Nakatani, J., Nakanishi, S., and Sasai, Y. (2000). *Xenopus* kielin: A dorsalizing factor containing multiple chordin-type repeats secreted from the embryonic midline. *Proc. Natl. Acad. Sci. USA* **97,** 5291–5296.

McMahon, J. A., Takada, S., Zimmerman, L. B., Fan, C. M., Harland, R. M., and McMahon, A. P. (1998). Noggin-mediated antagonism of BMP signaling is required for growth and patterning of the neural tube and somite. *Genes Dev.* **12,** 1438–1452.

Merino, R., Ganan, Y., Macias, D., Economides, A. N., Sampath, K. T., and Hurle, J. M. (1998). Morphogenesis of digits in the avian limb is controlled by FGFs, TGFbetas, and noggin through BMP signaling. *Dev. Biol.* **200,** 35–45. doi: 10.1006/dbio/1998.8946.

Merino, R., Rodriguez-Leon, J., Macias, D., Ganan, Y., Economides, A. N., and Hurle, J. M. (1999). The BMP antagonist Gremlin regulates outgrowth, chondrogenesis and programmed cell death in the developing limb. *Development* **126,** 5515–5522.

Nakashima, M., Toyono, T., Akamine, A., and Joyner, A. (1999). Expression of growth/differentiation factor 11, a new member of the BMP/TGFbeta superfamily during mouse embryogenesis. *Mech. Dev.* **80,** 185–189.

Nakayama, N., Fang, I., and Elliott, G. (1998). Natural killer and B-lymphoid potential in CD34+ cells derived from embryonic stem cells differentiated in the presence of vascular endothelial growth factor. *Blood* **91,** 2283–2295.

Nakayama, N., Lee, J., and Chiu, L. (2000). Vascular endothelial growth factor synergistically enhances bone morphogenetic protein-4-dependent lymphohematopoietic cell generation from embryonic stem cells *in vitro*. *Blood* **95,** 2275–2283.

Nifuji, A., and Noda, M. (1999). Coordinated expression of noggin and bone morphogenetic proteins (BMPs) during early skeletogenesis and induction of noggin expression by BMP-7. *J. Bone Miner. Res.* **14,** 2057–2066.

Nishinakamura, R., Matsumoto, Y., Matsuda, T., Ariizumi, T., Heike, T., Asashima, M., and Yokota, T. (1999). Activation of Stat3 by cytokine receptor gp130 ventralizes *Xenopus* embryos independent of BMP-4. *Dev. Biol.* **216,** 481–490. doi: 10.1006/dbio/1999.9518.

Ozaki, T., Ma, J., Takenaga, K., and Sakiyama, S. (1996). Cloning of mouse DAN cDNA and its down-regulation in transformed cells. *Jpn. J. Cancer Res.* **87,** 58–61.

Pappano, W. N., Scott, I. C., Clark, T. G., Eddy, R. L., Shows, T. B., and Greenspan, D. S. (1998). Coding sequence and expression patterns of mouse chordin and mapping of the cognate mouse chrd and human CHRD genes. *Genomics* **52,** 236–239.

Pathi, S., Rutenberg, J. B., Johnson, R. L., and Vortkamp, A. (1999). Interaction of Ihh and BMP/Noggin signaling during cartilage differentiation. *Dev. Biol.* **209,** 239–253. doi: 10.1006/dbio/1998.9181.

Pearce, J. J., Penny, G., and Rossant, J. (1999). A mouse cerberus/Dan-related gene family. *Dev. Biol.* **209,** 98–110. doi: 10.1006/dbio/1999.9240.

Piccolo, S., Agius, E., Lu, B., Goodman, S., Dale, L., and De Robertis, E. M. (1997). Cleavage of Chordin by Xolloid metalloprotease suggests a role for proteolytic processing in the regulation of Spemann organizer activity. *Cell* **91,** 407–416.

Piccolo, S., Sasai, Y., Lu, B., and De Robertis, E. M. (1996). Dorsoventral patterning in *Xenopus:* Inhibition of ventral signals by direct binding of chordin to BMP-4. *Cell* **86,** 589–598.

Podos, S. D., and Ferguson, E. L. (1999). Morphogen gradients-new insights from Dpp. *Trends Genet.* **15,** 396–402.

Sambrook, J., Fritsch, E. F., and Maniatis, T. (1989). "Molecular Cloning: A Laboratory Manual." Cold Spring Harbor Laboratory Press, Cold Spring Harbor, NY.

Sasai, Y., Lu, B., Steinbeisser, H., Geissert, D., Gont, L. K., and De Robertis, E. M. (1994). *Xenopus* chordin: A novel dorsalizing factor activated by organizer-specific homeobox genes. *Cell* **79,** 779–790.

Schulte-Merker, S., Lee, K. J., McMahon, A. P., and Hammerschmidt, M. (1997). The zebrafish organizer requires chordino. *Nature* **387,** 862–863.

Scott, I. C., Blitz, I. L., Pappano, W. N., Imamura, Y., Clark, T. G., Steiglitz, B. M., Thomas, C. L., Maas, S. A., Takahara, K., Cho, K. W., and Greenspan, D. S. (1999). Mammalian BMP-1/Tolloid-related metalloproteinases, including novel family member mammalian Tolloid-like 2, have differential enzymatic activities and distributions of expression relevant to patterning and skeletogenesis. *Dev. Biol.* **213,** 283–300. doi: 10.1006/dbio/1999.9383.

Scott, I. C., Steiglitz, B. M., Clark, T. G., Pappano, W. N., and Greenspan, D. S. (2000). Spatiotemporal expression patterns of mammalian chordin during postgastrulation embryogenesis and in postnatal brain. *Dev. Dyn.* **217,** 449–456.

Seidah, N. G., and Chretien, M. (1999). Proprotein and prohormone convertases: A family of subtilases generating diverse bioactive polypeptides. *Brain Res.* **848,** 45–62.

Shawlot, W., Deng, J. M., and Behringer, R. R. (1998). Expression of the mouse cerberus-related gene, Cerr1, suggests a role in anterior neural induction and somitogenesis. *Proc. Natl. Acad. Sci. USA* **95,** 6198–6203.

Shi, Y.-P., Mohapatra, G., Miller, J., Hanahan, D., Lander, E., Gold, P., Pinkel, D., and Gray, J. (1997). FISH probes for mouse chromosome identification. *Genomics* **45,** 42–47.

Smith, D. M., Nielsen, C., Tabin, C. J., and Roberts, D. J. (2000). Roles of BMP signaling and Nkx2.5 in patterning at the chick midgut-foregut boundary. *Development* **127,** 3671–3681.

Smith, W. C., and Harland, R. M. (1992). Expression cloning of noggin, a new dorsalizing factor localized to the Spemann organizer in *Xenopus* embryos. *Cell* **70,** 829–840.

Solloway, M. J., Dudley, A. T., Bikoff, E. K., Lyons, K. M., Hogan, B. L., and Robertson, E. J. (1998). Mice lacking Bmp6 function. *Dev. Genet.* **22,** 321–339.

Stanley, E., Biben, C., Kotecha, S., Fabri, L., Tajbakhsh, S., Wang, C. C., Hatzistavrou, T., Roberts, B., Drinkwater, C., Lah, M., Buckingham, M., Hilton, D., Nash, A., Mohun, T., and Harvey, R. P. (1998). DAN is a secreted glycoprotein related to *Xenopus* cerberus. *Mech. Dev.* **77,** 173–184.

Sukegawa, A., Narita, T., Kameda, T., Saitoh, K., Nohno, T., Iba, H., Yasugi, S., and Fukuda, K. (2000). The concentric structure of the developing gut is regulated by Sonic hedgehog derived from endodermal epithelium. *Development* **127,** 1971–1980.

Takahashi, N., and Ko, M. S. H. (1994). Toward a whole cDNA catalog: Construction of an equalized cDNA library from mouse embryos. *Genomics* **23,** 202–210.

Takebe, Y., Seiki, M., Fujisawa, J., Hoy, P., Yokota, K., Arai, K., Yoshida, M., and Arai, N. (1988). SR alpha promoter: an efficient and versatile mammalian cDNA expression system composed of the simian virus 40 early promoter and the R-U5 segment of human T-cell leukemia virus type 1 long terminal repeat. *Mol. Cell. Biol.* **8,** 466–472.

Topol, L. Z., Marx, M., Laugier, D., Bogdanova, N. N., Boubnov, N. V., Clausen, P. A., Calothy, G., and Blair, D. G. (1997). Identification of drm, a novel gene whose expression is suppressed in transformed cells and which can inhibit growth of normal but not transformed cells in culture. *Mol. Cell. Biol.* **17,** 4801–4810.

Wang, E. A. (1993). Bone morphogenetic proteins (BMPs): Therapeutic potential in healing bony defects. *Trends Biotechnol.* **11,** 379–383.

Wilcox, J. N. (1993). Fundamental principles of in situ hybridization. *J. Histochem. Cytochem.* **41,** 1725–1733.

Wozney, J. M., Capparella, J., and Rosen, V. (1993). The bone morphogenetic proteins in cartilage and bone development. *In* "Molecular Basis of Morphogenesis" (M. Bernfield, Ed.), pp. 221–230. Wiley–Liss, New York.

Yu, K., Srinivasan, S., Shimmi, O., Biehs, B., Rashka, K. E., Kimelman, D., O'Connor, M. B., and Bier, E. (2000). Processing of the *Drosophila* Sog protein creates a novel BMP inhibitory activity. *Development* **127,** 2143–2154.

Zhao, R., Lawler, A. M., and Lee, S. J. (1999). Characterization of GDF-10 expression patterns and null mice. *Dev. Biol.* **212,** 68–79. doi: 10.1006/dbio/1999.9326.

Zimmerman, L. B., De Jesus-Escobar, J. M., and Harland, R. M. (1996). The Spemann organizer signal noggin binds and inactivates bone morphogenetic protein 4. *Cell* **86,** 599–606.

Received for publication September 11, 2000
Accepted January 23, 2001
Published online March 16, 2001